

## HiSST: 4th International Conference on High-Speed Vehicle Science Technology 22 -26 September 2025, Tours, France



# Applying Uncertainty Quantification to Thermal Protection System Design for a Hypersonic Point-to-Point Passenger Vehicle

Jascha Wilken<sup>1</sup>, Dr. Aaron D. Koch<sup>2</sup>

#### **Abstract**

Thermal Protection System (TPS) design is a critical challenge for hypersonic vehicles, where the system must withstand extreme reentry heating without adding excessive mass. Conventional methods often rely on conservative assumptions, which can lead to overdesigned systems. This paper takes a first exploratory step toward incorporating uncertainty quantification into TPS design, using the SpaceLiner point-to-point passenger transport concept as a reference case.

A toolchain was implemented that combines trajectory optimization, aerothermal database generation, and simplified TPS sizing to explore the influence of input uncertainties. The study considers variations in lift and drag coefficients, velocity, flight path angle, altitude, and the transition Reynolds number. Using Sobol sampling, 512 trajectories were generated and analyzed to estimate impacts on TPS mass and regional distribution.

As expected, the results suggest that uncertainties in the heat flux estimation and the transition to turbulent flow exert the largest influence on TPS design, while initial altitude plays only a minor role. Some outcomes are counterintuitive: For example, reduced velocity or higher drag lead to lower-altitude trajectories, increasing thermal loads and TPS mass. Clustering analysis further reveals distinct groups of trajectories and TPS results, underscoring the coupled nature of the problem.

Overall, the work demonstrates how uncertainty quantification can provide additional insight into the sensitivity of TPS design. While simplified, this approach highlights key drivers and trade-offs, and points toward more balanced methods for future hypersonic vehicle studies.

**Keywords:** thermal protection system, hypersonic transport, uncertainty quantification, trajectory optimization, SpaceLiner

#### 1. Introduction

The design of a Thermal Protection System (TPS) for atmospheric reentry vehicles is a critical challenge in aerospace engineering. The extreme heat generated during reentry, caused by aerodynamic heating, requires the TPS to shield the vehicle and its payload from catastrophic failure. The TPS design must balance thermal efficiency, structural integrity, and minimal mass to ensure mission success while optimizing payload capacity. One of the significant challenges in TPS design is accounting for uncertainties in vehicle parameters and environmental conditions, which can significantly affect reentry dynamics and heat loads.

Ideally, the uncertainties along the entire design process are included, not only uncertainties specific to the TPS. For example, an error in the MECO position might require the GNC to select a different

<sup>&</sup>lt;sup>1</sup> Space Launcher Systems Analysis, Institute of Space Systems, Deutsches Zentrum für Luft- Und Raumfahrt (DLR), Bremen, Germany, jascha.wilken@dlr.de

<sup>&</sup>lt;sup>2</sup> Space Launcher Systems Analysis, Institute of Space Systems, Deutsches Zentrum für Luft- Und Raumfahrt (DLR), Bremen, Germany

trajectory, which will result in a different aerothermal environment and a different spatial and temporal location of the laminar/turbulent transition.

Commonly, worst case assumptions are used to design the various subsystems in order to arrive at a robust design. However, taken to the extreme for every aspect of the vehicle, this can result in overly conservative solutions.

In order to characterize the impact of selected uncertainties on the TPS design and final mass, a toolchain is employed that combines trajectory optimization, aerothermal database generation and final TPS sizing to quantify their impact.

Apart from this motivation, the inspection of the design problem from this perspective shall also allow a deeper understanding of the sizing factors and the interactions between the selected subsystems and their effect on the total system.

As a reference vehicle, the upper stage of the SpaceLiner point-to-point passenger transport system is chosen. The study considers a reference mission traveling westward along the equator, a scenario that pushes the vehicle to the limits of its performance capabilities.

#### 2. Methods

#### 2.1. Reference configuration

The SpaceLiner is a fully reusable, rocket propelled, hypersonic passenger transport concept under investigation at DLR. An overview over the current status and recent advances is given in [1]. For this study the focus lies on the upper stage, specifically the newly updated geometry for the 8<sup>th</sup> iteration [2]. The new geometry, as well as the previous shape of the SpaceLiner 7 orbiter are shown in Figure 1.

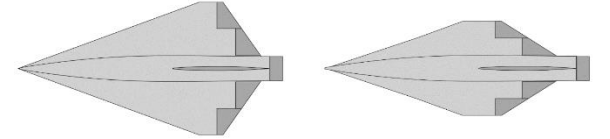


Figure 1: Sketches of the SLO7 (left) and the SLO8 candidate geometry (right)

The passenger transport passenger mission is a point-to-point mission, that has to consider thermal, mechanical as well as regulatory constraints. Populated areas are to be avoided for safety reasons but also to minimize the impact of the sonic boom. Examples of full trajectories and their optimization are shown in [3].

For this work a simplified reference mission is used, which consists of travelling westward along the equator for ca. half a circumference, specifically 175°. Due to the Earth's rotation this mission is far more challenging than the equivalent distance eastward [4].

#### 2.2. Trajectory optimization

The same tools for trajectory optimization as in [3] and [4] are used. The DLR-SART trajectory simulation tool *tosca* is wrapped in python code and the pymoo library [5] is used for optimizing the trajectories, in this case specifically the single-objective Differential Evolution [6] algorithm.

The single objective in this study is a combination of the maximum estimated stagnation point heat flux as well as its integral, which can be evaluated with analytical formulas within the trajectory simulation itself. The two components are weighed so that the maximum stagnation point heat flux dominates the final objective, with the integral contributing about 4%.

Based on a reference trajectory where both ascent and descent are optimal, uncertainties are applied to the final engine cut-off conditions. Then, based on the new separation state, the descent is optimized. A special aspect of the mission is the required downrange performance. So, if for example, the gliding distance is degraded by reduced lift generation, the optimization has to compensate for this by the angle of attack profile. Usually, this leads to higher heat loads, which will be discussed in the results in chapter 3.

#### 2.3. Aerothermal Database

The heat flux encountered during the flight depends not only on the aerodynamic environment, but also on the current wall temperature. As the actual wall temperature during the flight is unknown a

priori, the AETDB has to be generated for each timepoint, surface element and wall temperature, allowing for interpolation during the subsequent TPS design simulations. The surface inclination method-based code HOTSOSE [7] is iteratively called to generate the required database.

The transition from laminar to turbulent flow is assumed to be instantaneous at a given Reynolds number. In reality, the transition is gradual and can contain local hotspots [8]. The determination of the exact conditions at which the flow becomes turbulent remains challenging and depends on the specific flow conditions as well as the geometry of the vehicle in question. In this specific use case, it may be further complicated by the active cooling of the leading edge via transpiration cooling, which can trigger an early transition for the areas behind the actively cooled area. Internal active cooling via spray cooling could mitigate this issue. Further discussion on the different possibilities of actively cooling the leading edge can be found in [9].

A fixed transition Reynolds number is used here to highlight design impact, without attempting to capture the full complexity of transition.

#### 2.4. Thermal Protection System

The TPS for each trajectory sample is assessed with the DLR-SART tool *top3*. In order to size the TPS for an entire vehicle with an acceptable amount of computational effort, a number of assumptions are made. Local masses such as standoffs are not implicitly considered, but have to be explicitly considered by the engineer performing the analysis.

In order to allow for fairly quick parameter or Monte Carlo studies, the thermal state of the vehicle is not evaluated in 3D but instead at critical points via 1D thermal conduction models. The analysis is done along the following steps:

- 1) Sorting surface elements in regions of identical TPS
  - a) Based on the generated AETDB, for each surface element the maximal radiation-adiabatic equilibrium temperature is calculated.
  - b) According to the surface temperature limits determined by the user, surface elements are sorted into temperature regions based on the maximal equilibrium temperature.
- 2) Sizing of each TPS region
  - a) For each region, the surface element with the highest heat flux integral over the mission is identified.
  - b) Isolation thickness optimization for each region
    - i) Via 1D heat conduction simulations the maximal temperature behind the isolation layer is determined.
    - ii) The thickness of the isolation layer is minimized, while still respecting the thermal constraints of the vehicle structure.

It is important to note, that a region is entirely defined by the peak expected surface temperature and is not connected to geometrical features. When comparing the TPS resulting from two different reentry trajectories the same temperature region might cover very different parts of the vehicle, depending on the velocity, altitude and angle of attack profile flown in each case.

The reference TPS architecture and the results for selected trajectories are discussed in [1]. For the specific calculations done herein, the following stacks and temperature regions were used:

- AFRSI, <620 K</li>
- AFRSI, 760 K 620 K
- TABI, 900 K 760 K
- TABI, 1125 K 900 K
- TUFI, 1280 K 1125 K
- TUFI, 1580 K 1280 K
- CMC, 1830 K 1580 K
- CMC, 1890 K 1830 K
- CMC, >1890 K

The last and hottest region likely reaches temperatures where the reusability of CMC is questionable. This is the region that would be actively cooled in the actual vehicle design. For this study, it is simplified to a separate passively cooled region. The results show the total area that has to be actively cooled and indicate the total heat load entering the TPS.

As each region shares a TPS thickness, multiple regions with the same TPS stack allow for some mass optimization by having different isolation thicknesses. Optimizing each panel individually would be mass optimal, but adds substantial complexity to the production.

## 2.5. Uncertainty quantification

The effect of six uncertainties is explored herein:

- Lift coefficient
- Drag coefficient
- Initial Velocity
- Initial Flight Path Angle (FPA)
- Initial Altitude
- Transition Reynolds number
- Heat Flux

Table 1: Considered uncertainties including reference values. All sampled uniformly.

Parameter	Reference value	Assumed uncertainty
Lift coefficient	Depends on flight point	±5%
Drag coefficient	Depends on flight point	±5%
Initial velocity	8 km/s	±30 m/s
Initial FPA	0	±0.25 °
Initial Altitude	75 km	±0.2 km
Transition Reynolds	1e6	x [1-10]
number		
Heat flux	Depends on flight point	± 10%

The values were chosen to reflect possible, but conservative deviations from the reference values. For example, the uncertainty in the final velocity reflects about ~1s variation in the exact engine cut-off. In order to illustrate the effect, larger values were chosen when in doubt. For many of these, especially the altitude, it is likely that the GNC system can achieve significantly higher accuracy during ascent. However, as the SpaceLiner hardly leaves the atmosphere, the final uncertainties might be larger than for conventional launch vehicles. These can use long exo-atmospheric phases to correct any errors aggregated through atmospheric influences.

For the transition Reynolds number, the uncertainty is chosen as very large to represent the actual uncertainty in the current modelling. Also, only the effect on the aerothermal loads is evaluated, changes in the aerodynamic performance caused by earlier or later transition are not considered herein.

A total of 512 samples were generated using Sobol sampling and analyzed. For each sample first an optimal trajectory was identified, the corresponding aerothermal database generated and finally the TPS sized. The computational effort associated with these steps precludes the generation of significantly larger sample sizes.

#### 3. Results

### 3.1. Total TPS mass

Figure 2 shows the effect the various uncertainties have on the final mass of the TPS. This result is purely theoretical, as the TPS cannot be reconfigured on the fly, but it shows the effect the various uncertainties have on the required TPS mass.

Figure 2: Effect of uncertainties on TPS total mass

At first glance, the uncertainty in the flight path angle, the transition Reynolds number and the heat flux have the largest impact. The initial altitude seems to have little to no impact. It is noteworthy that while the Reynolds transition number is varied by an order of magnitude, the impact is not an order of magnitude larger than the smaller overall uncertainty in the heat flux estimation.

Some trends appear that are specific to the vehicle type and its mission: For a reentry vehicle it can be expected that higher drag and lower initial velocity would lead to reduced TPS masses, however the opposite is the case here. In order to still fulfill its mission, the vehicle has to fly at lower angles of attack, which offer higher L/D ratios but also result in flight at lower altitudes, which in turn leads to higher heat fluxes. This will be discussed in more detail in section 3.6. A formal sensitivity analysis of the various input and output parameters is discussed in section 3.5. The apparent noise in the results is also discussed therein.

#### 3.2. TPS CoG-X position

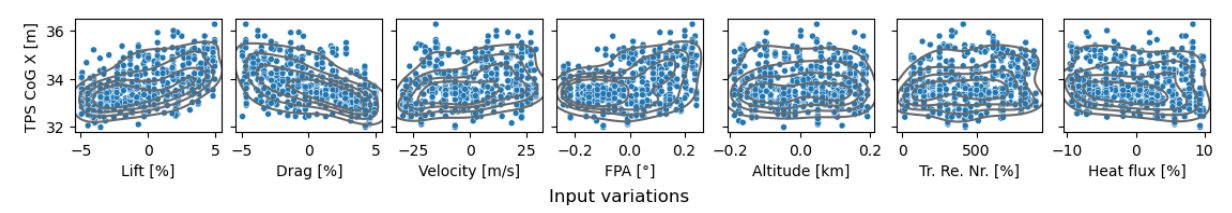


Figure 3: Effect of uncertainties on TPS X-CoG position

For the design of the entire vehicle not only the TPS mass, but also its center of gravity position is of interest. The position along the vehicle axis (here X-axis) is of special interest. Figure 3 shows the impact of the input uncertainties on this result. Here the changes in lift and drag coefficients appear to have the largest impact, possibly because they result in different angle of attack profiles during high heat flux phases.

## 3.3. Clustering analysis

In order to better categorize the different results herein and in the following analysis of the individual TPS regions, the k-means clustering algorithm was applied to separate the dataset into three distinct groups. All output variables of the TPS design were used for the classification: The total mass as well as the surface area and density of each TPS region. A higher number of clusters would yield additional insights or relevant subgroups; however, discussion of all cases would be beyond the scope of this paper. Thus, a small number that still can represent the key cases was chosen for the following discussion.

Figure 4 shows the distribution of the three clusters over the input parameters, while Figure 5 shows the cluster in relation to the final TPS mass. Cluster #2, shown in orange clearly consists of all cases where the transition Reynolds numbers are low. The samples in cluster #1, in blue, represent the cases in which the changed initial conditions lead to unfavorable trajectories and thus higher TPS masses. Cluster #3 (in green) consists of the more benign cases, with small deviations from the reference or deviations that end up being beneficial.

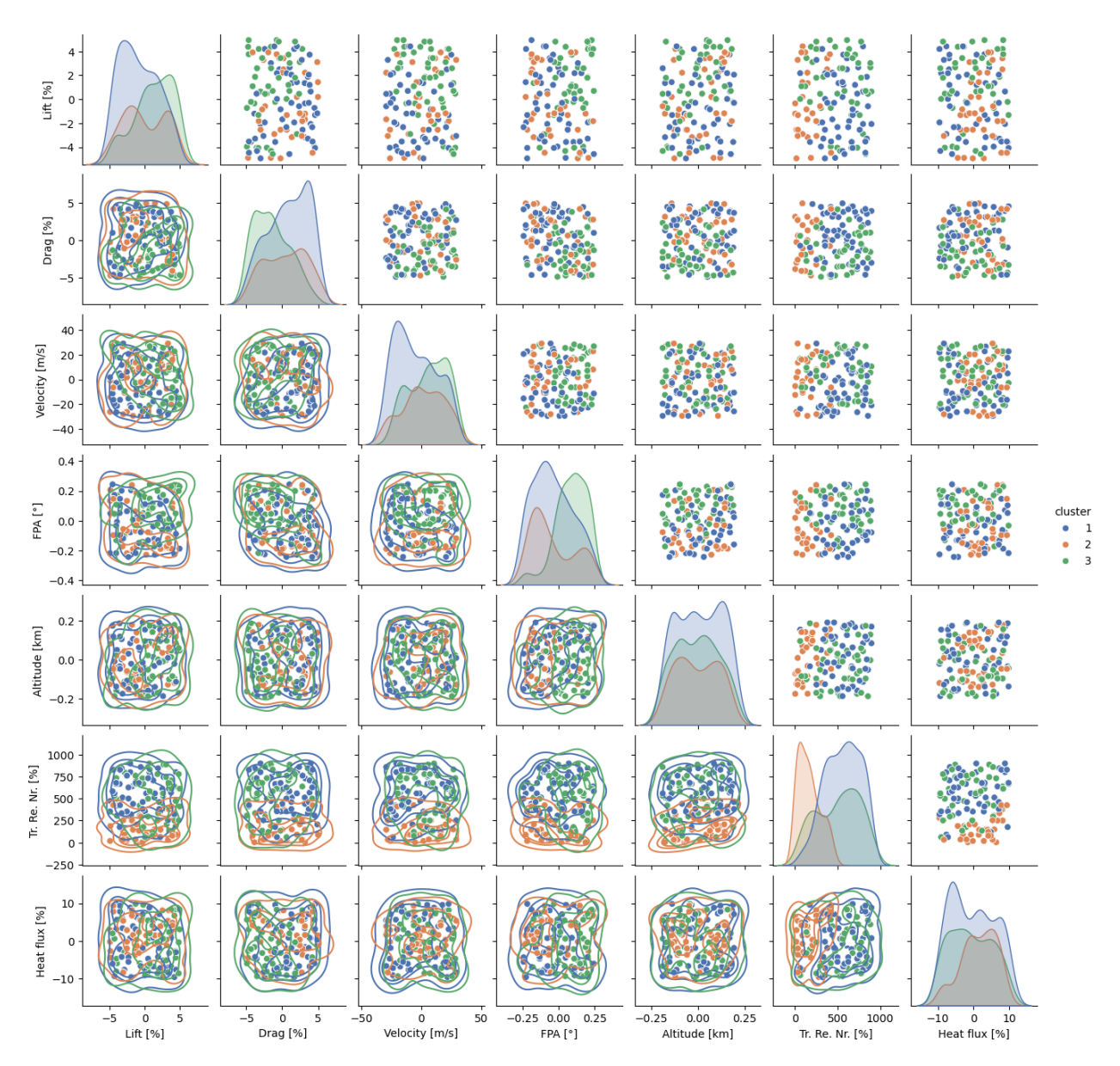


Figure 4: Distribution of clustered results over input uncertainties

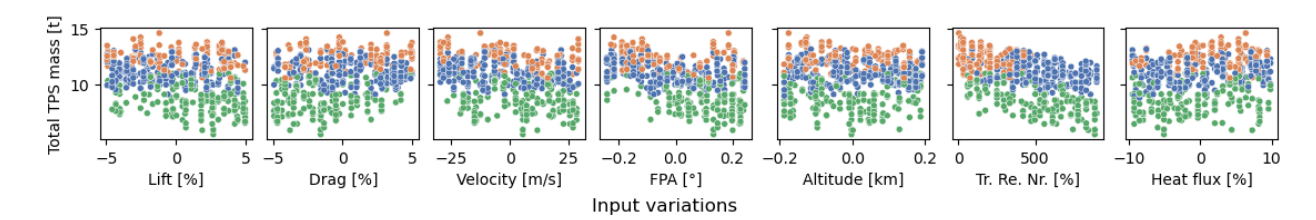


Figure 5: Effect of uncertainties on TPS total mass, colored by cluster (1: blue, 2: orange, 3: green)

#### 3.4. Size and mass of TPS regions

As the location of the TPS regions are assigned depending on the local maximum surface temperature, the distribution shifts from case to case as well as the thickness of the individual regions. As in these cases there are nine different regions, a total of 18 different outputs can be considered. For this paper the focus here will lie on the surface area of each region, shown in Figure 6. In the figure the clusters are also indicated by color.

The size of the individual regions varies substantially, often by orders of magnitude. While the region distribution of cluster #2 (in orange) often varies substantially from the other clusters, there also are regions where the clusters #1 and #3 show clear differences, e.g. in region #3.

When looking at the individual regions, the impact of the transition Reynolds number on the area of each region (which depend on the peak surface temperature) varies depending on the approximate location of the regions. For the higher temperature regions, usually covering smaller areas at the front of the vehicle, only smaller transition Reynolds numbers have an impact, as for higher values these forward areas remain laminar. The range over which a change in transition Reynolds number causes a change in the region area shifts visibly as it approaches the usually rearward located areas with lower surface temperature, e.g. region #1 and #2.

The interpretation of some patterns remains tentative, especially regions #3 and #5 show a lot of noise. While they show some sensitivity to the clusters, there are large variations without clear attribution to any of the input uncertainties. This might be caused by some variation in the angle of attack profile (see also section 3.5) or could also by the "migration" into and from adjacent area regions, which might obfuscate the trends.

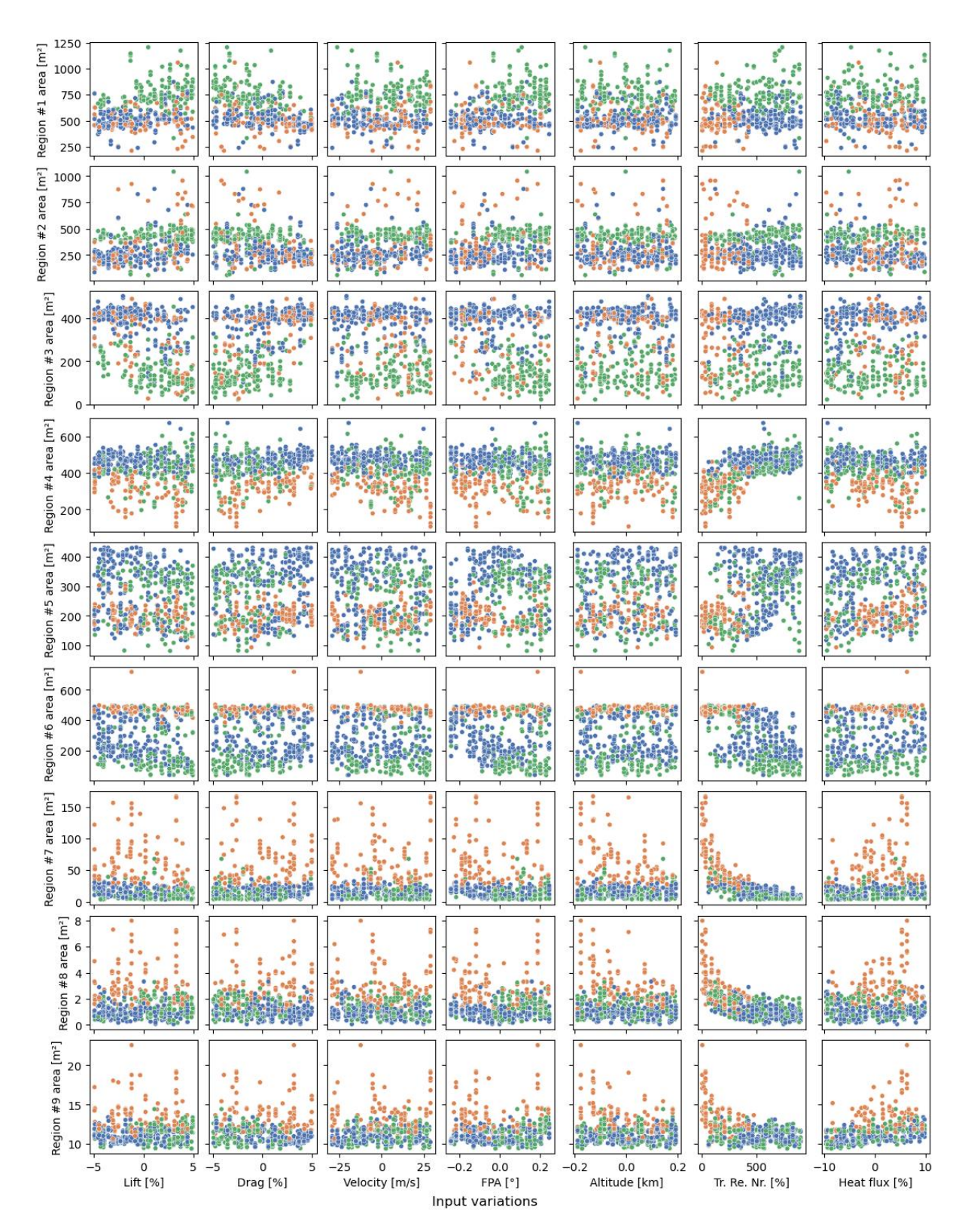


**Figure 6:** Area distribution of TPS regions depending on investigated uncertainties, colored by cluster (1: blue, 2: orange, 3: green)

HiSST-2025-0066 8 Jascha Wilken, Aaron D. Koch

#### 3.5. Sensitivity analysis

Global sensitivities were evaluated via High-Dimensional Model Representation (HDMR) [10]. With this method a surrogate model was generated and the contributions of the input variables to the variability of the output quantified. In Figure 7 independent, correlated and total sensitivity indices for the impact of the input uncertainties on the total TPS mass and CoG x position are shown.

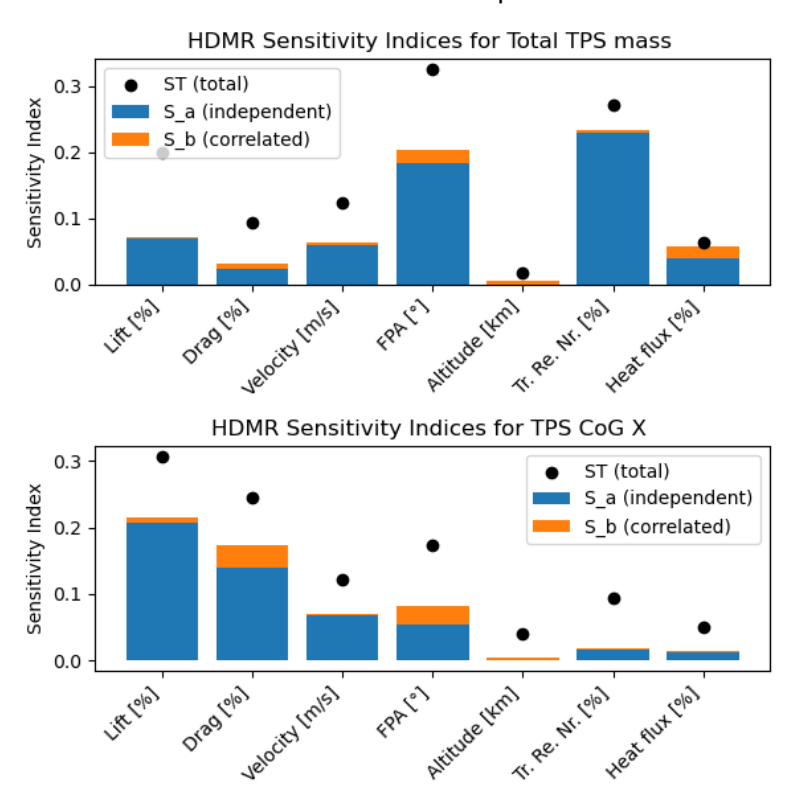


Figure 7: Sensitivity Indices for TPS mass and CoG x-position

As already visible in the raw sample results, the total mass of the TPS is most sensitive to the transition Reynolds number and the initial flight path angle. The uncertainties in the heat flux calculation, lift coefficient and velocity are of similar magnitude.

The total sensitivity indices exceed the sum of independent and correlated terms, indicating noise in the results. One possible source of this noise might be the trajectory optimization objective. Therein, only the stagnation heat flux is considered but not the angle of attack the vehicle has in each moment. As the angle of attack influences the heat flux (especially on the large surface areas below the vehicle) it also impacts the TPS regions. For example, flying at high angles of attack at certain moments in the trajectory may lead to large areas experiencing higher heat fluxes than otherwise. It is not trivial to consider this in the trajectory optimization, as any objective function has to be calculated quickly, so the runtime doesn't increase excessively. One possibility might be the consideration of the product of angle of attack and heat flux, similarly to structural loads being correlated with the product of dynamic pressure and angle of attack. This has not been further investigated within the scope of this study.

#### 3.6. Trajectory results

The mean values and standard deviation of the trajectories of each cluster discussed above are shown in Figure 8.

The trends in the clusters discussed above can be seen therein. Generally, the trajectories of cluster #3 (in green) fly at higher altitudes, specifically in the middle part of the trajectory. This leads to lower total peak heat flux as well as integral heat load. This is achieved by flying at higher angles of attack, which don't deliver optimal L/D ratios, but since these are the cases with errors benefiting the range performance, the target range is still reached. Conversely, the cases in cluster #1 (blue), need to fly at lower angles of attack to achieve the mission, which results in higher heat fluxes and loads.

HiSST-2025-0066 Page |

9

In general, the stagnation point heat flux varies to a stronger degree than other trajectory parameters, the peak values vary from 1.2-1.8 MW/m<sup>2</sup>.

The angle of attack profile in the final phase of the trajectory often shows some variation, this is due to the final portion of the flight not being particularly relevant to the optimization goal. The heat fluxes are already very low, so that there is no strong selection pressure within the genetic optimization towards a specific value, as long as the vehicle reaches the target downrange distance.

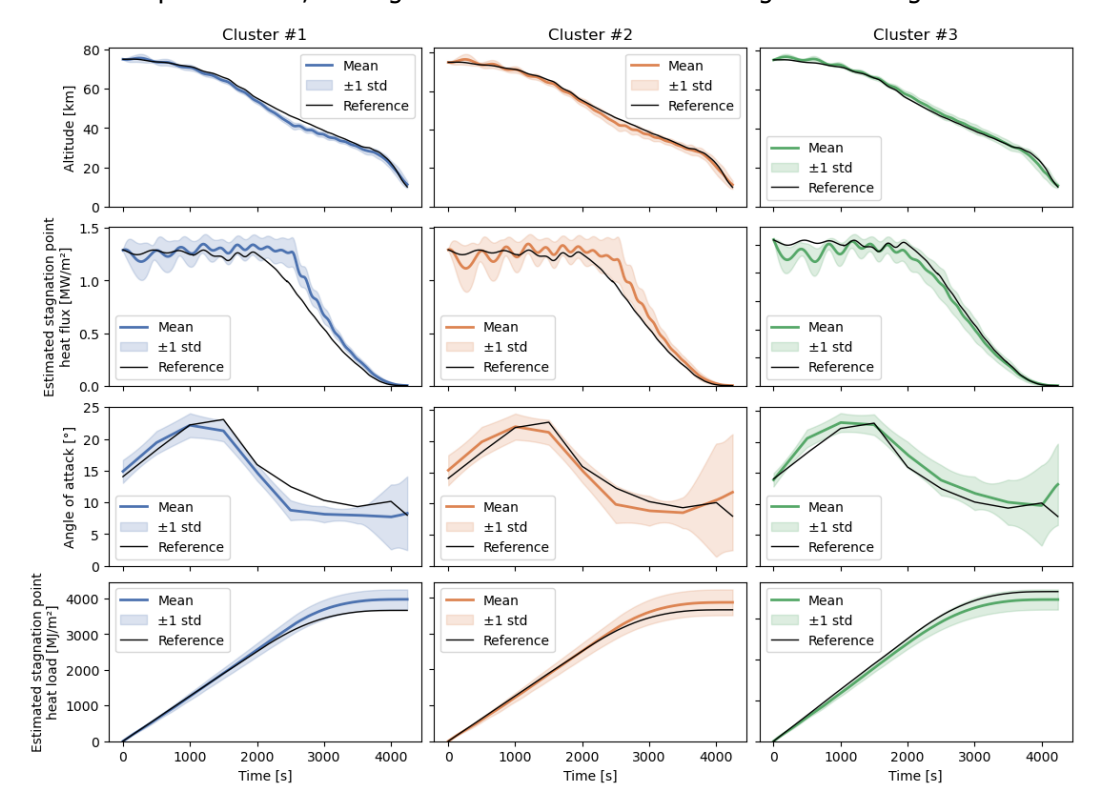


Figure 8: Sampled trajectory parameters over time, grouped by cluster (1: blue, 2: orange, 3: green)

In the trajectory optimization, only the estimated stagnation point heat flux is considered. This theoretical value can be quickly estimated with a parametric equation during the optimization and, by definition always assumes laminar flow. However, as the transition to turbulent flow has such a large impact, in the future the boundary transition point might also be considered and, if possible, postponed by flying at higher altitudes even at lower velocities. In some work on TPS design, such boundaries have been previously discussed and included, for example in [11].

HiSST-2025-0066 10 Jascha Wilken, Aaron D. Koch

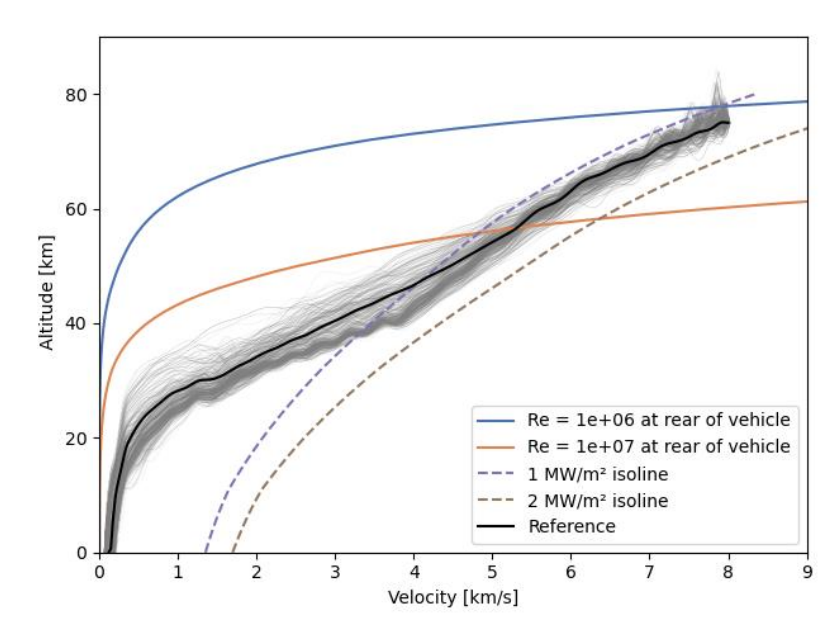


Figure 9: Altitude-Velocity profile for sampled trajectories, with isolines for stagnation point heat flux and transition onset

Figure 9 shows the altitude velocity profile of the sampled trajectories with iso-lines for turbulence onset and stagnation point heat flux. Due to the large uncertainty, the onset at the rear of the vehicle is shown for Reynolds numbers of 10^6 and 10^7. It can be seen that the optimizer chooses trajectories that fly in parallel to the iso-heat flux lines, which essentially results in the, relatively, constant heat fluxes seen in Figure 8. It can also be seen that the iso-lines for the transition onset follow different trends and that the vehicle crosses a large range of Reynolds numbers during the flight. As the stagnation point heat fluxes remain high down to ca. 4 km/s, turbulent flow in this phase leads to the actual heat flux being highest at these timepoints. This mainly affects cooler TPS regions, since the leading edge remains laminar during peak heating.

#### 4. Conclusion & Outlook

This study applied uncertainty quantification to the design of the thermal protection system for the SpaceLiner hypersonic passenger vehicle. By coupling trajectory optimization, aerothermal database generation, and TPS sizing, the influence of six key uncertainties on TPS mass, center of gravity, and regional distribution was assessed. The analysis showed that the transition Reynolds number and the initial flight path angle are the dominant drivers, while altitude has little effect. Counterintuitive trends, such as increased TPS mass at lower velocities, underline the tight coupling between aerodynamics, trajectory, and thermal loading.

Beyond specific findings, the work demonstrates that uncertainty quantification can reveal sensitivities and trade-offs that are obscured by conservative worst-case assumptions. Incorporating such methods early in design can help avoid over-sizing, improve system balance, and guide where more accurate models or measurements are most critical. Future work should extend the approach to larger sample sizes, refined turbulence transition models as well as improved trajectory optimization objectives.

#### References

- [1] Sippel, M. et al: SpaceLiner: the 2025 pre-definition status report. 4<sup>th</sup> International Conference on High-Speed Vehicle Science Technology, September 2025, Tour, France
- [2] Mauriello, Tommaso und Wilken, Jascha und Callsen, Steffen und Bussler, Leonid und Sippel, M.: Multidisciplinary design analysis and optimization of the aerodynamic shape of the SpaceLiner passenger stage. Acta Astronautica. Elsevier. 2024. doi: 10.1016/j.actaastro.2024.07.054 . ISSN 0094-5765.

- [3] Callsen, S., Wilken, J. & Sippel, M. Analysis of sonic boom propagation and population disturbance of hypersonic vehicle trajectories. CEAS Space J 17, 797–814 (2025). https://doi.org/10.1007/s12567-024-00583-7
- [4] Wilken, J., Callsen, S. Mission design for point-to-point passenger transport with reusable launch vehicles. CEAS Space J 16, 319–332 (2024). <a href="https://doi.org/10.1007/s12567-023-00498-9">https://doi.org/10.1007/s12567-023-00498-9</a>
- [5] J. Blank and K. Deb, pymoo: Multi-Objective Optimization in Python, in IEEE Access, vol. 8, pp. 89497-89509, 2020, doi: 10.1109/ACCESS.2020.2990567
- [6] Kenneth Price, Rainer M. Storn, and Jouni A. Lampinen. Differential Evolution: A Practical Approach to Global Optimization (Natural Computing Series). Springer-Verlag, Berlin, Heidelberg, 2005. ISBN 3540209506
- [7] Reisch, U., and Th Streit. Surface inclination and heat transfer methods for reacting hypersonic flow in thermochemical equilibrium. New Results in Numerical and Experimental Fluid Mechanics: Contributions to the 10th AG STAB/DGLR Symposium Braunschweig, Germany 1996. Wiesbaden: Vieweg+ Teubner Verlag, 1997.
- [8] Cunbiao Lee, Shiyi Chen, Recent progress in the study of transition in the hypersonic boundary layer, *National Science Review*, Volume 6, Issue 1, January 2019, Pages 155–170, <a href="https://doi.org/10.1093/nsr/nwy052">https://doi.org/10.1093/nsr/nwy052</a>
- [9] Schwanekamp, Tobias: System studies on active thermal protection of a hypersonic suborbital passenger transport vehicle. 19th AIAA International Space Planes and Hypersonic Systems and Technologies Conference. 2014.
- [10] Genyuan Li, H. Rabitz, P.E. Yelvington, O.O. Oluwole, F. Bacon, C.E. Kolb, and J. Schoendorf, "Global Sensitivity Analysis for Systems with Independent and/or Correlated Inputs", Journal of Physical Chemistry A, Vol. 114 (19), pp. 6022 6032, 2010, https://doi.org/10.1021/jp9096919
- [11] Wurster, K. E.: An assessment of the impact of transition on advanced winged entry vehicle thermal protection system mass. In: *16th Thermophysics Conference*. 1981. S. 1090.